International Journal of Heat and Mass Transfer 52 (2009) 665–669

Contents lists available at ScienceDirect

International Journal of Heat and Mass Transfer

journal homepage: www.elsevier.com/locate/ijhmt

Thermal conductivity of a clay-based aerogel

S.R. Hostler [a], A.R. Abramson [a,*], M.D. Gawryla [b], S.A. Bandi [b], D.A. Schiraldi [b]

[a] Department of Mechanical and Aerospace Engineering, Case Western Reserve University, 10900 Euclid Avenue, Cleveland, OH 44106, USA
[b] Department of Macromolecular Science and Engineering, Case Western Reserve University, 10900 Euclid Avenue, Cleveland, OH 44106, USA

ARTICLE INFO

Article history:
Received 9 February 2008
Received in revised form 10 April 2008
Available online 6 September 2008

Keywords:
Aerogel
Clay
Thermal conductivity
Effective medium

ABSTRACT

Aerogel materials exhibit superior thermal insulation characteristics due largely to their highly porous internal structure. A recently developed class of montmorillonite clay-based aerogels provides the attractive thermal properties of traditional aerogel materials using constituents that are chemically benign and abundantly available. Results are compared for aerogels made from clay alone and those with polyvinyl alcohol introduced during processing. Results demonstrate that as well as strength advantages, the addition of the polymer also leads to a reduction in thermal conductivity. Experimental thermal conductivity data as well as a model to describe the mechanisms involved in impeding thermal transport are presented.

1. Introduction

Aerogels are a class of materials largely composed of air with bulk densities in the 0.01–0.1 g/cm^3 range. These materials, among the least dense forms of solid matter, were first described by Kistler, who reported their preparation from silica [1]. On account of their extremely porous nature, aerogels show great promise for application in thermal insulation. Recent work has demonstrated the use of silica-based aerogels for both terrestrial and extraterrestrial insulation. Earth-based applications have focused on introducing solid [2] or granular [3] aerogel into building windows. Aerogel placed between the panes of a typical window provides an effective thermal barrier while still allowing for transmission of sunlight. Aerogel materials have also been used by NASA for a number of missions [4,5]. Aerogels can be formed in place from the gel state so they can be used to fill around complicated structures. This fact, combined with their low weight, make aerogel materials desirable for space-based applications. As a result of their high porosity, the mechanical strength of aerogel materials is low and these materials are quite delicate. This low strength is not a problem when aerogels are used to fill around a more rigid structure. To use aerogels as actual structural elements more internal rigidity is needed.

Though most aerogels are based on silica, recent work has shown the ability to create similar porous structures with different constituent materials. One promising substitute is clay. The abundance of clay and its limited toxicity make it particularly attractive. The earliest work detailing the freeze-drying of clay hydrogels was reported by Mackenzie [6] and Call [7]. The presence of opposite surface and edge charges in clays has been proposed as the cause of the unique structure created upon freeze-drying [8]. Individual clay particles link edge-to-face in a manner akin to a "house of cards." Since these early studies, considerable work has been done to stabilize these structures by varying solvents, surfactants, and other processing conditions [9–12]. Nonetheless, the clay aerogel (AeroClay®) samples in the present study achieve a stable structure without solvents or surfactant. They are derived from a solution of montmorillonite clay and water alone, minimizing toxicity concerns about the aerogel and the procedure used to produce it. Although the structure is stable, its mechanical strength is low. The addition of a polymer during processing improves the mechanical rigidity [11] to a point at which the clay-based aerogel sample is capable of supporting pressures on the order of 200 Pa without significant compression. In this work we investigate the thermal conductivity of these clay aerogel materials in two different orientations and further examine how the addition of the polymer influences thermal transport. Experimental data of thermal conductivity along with a complementary analytical model provides insight into thermal transport in these aerogel systems and how to tailor their structure to control their thermal properties.

2. Approach

2.1. Synthesis and structural characterization

The aerogel samples are made through a freeze-drying process similar to that described in Ref. [11,12]. Sodium-exchanged montmorillonite clay (Nanocor, Inc. \PGW) is mixed with deionized water in a Waring laboratory mixer for 1 min (3 wt% clay). This

* Corresponding author. Tel.: +1 216 368 4191; fax: +1 216 368 3007.
E-mail address: alexis.abramson@case.edu (A.R. Abramson).

0017-9310/$ - see front matter © 2008 Elsevier Ltd. All rights reserved.
doi:10.1016/j.ijheatmasstransfer.2008.07.002

Nomenclature

A	cross-sectional area
B	sample depth
d	clay sheet thickness
H	distance between clay sheets
k	thermal conductivity
K	extinction coefficient
L	thickness
n	refractive index
Q	rate of heat transfer
W	clay repeat cell width

Greek symbols

ΔT	temperature difference
ρ	density
σ	Stefan–Boltzmann constant

Subscripts

0	reference material
a	air
c	clay
eff	effective value
H	horizontally aligned sample
S	sample
rad	radiative
tot	total values for effective conductivity model
V	vertically aligned sample

solution is then placed in a 7.6 × 7.6 × 3.8 cm mold constructed of poly(tetrafluoroethylene) sides/aluminum bottom, contacting the bottom of the mold with liquid nitrogen until the sample is completely frozen. The frozen mold and sample is then placed on a Labconco freeze drier, vacuum is applied, and the sample sublimed over 36–48 h. The resulting structure, shown in Fig. 1, consists of thin sheets of clay stacked in parallel with a limited number of struts between the sheets. During freezing, the clay sheets align with the direction of the ice front that propagates through the mixture. The density of the aerogel samples is around 50 kg/m^3 compared to 2350 kg/m^3 for bulk montmorillonite clay. The resulting aerogel specimens employed in this study were 7.6 cm square and approximately 0.6 cm thick.

The clay aerogel samples are frozen and subsequently sublimed in two different orientations relative to the flat faces of the samples. These orientations are depicted in Fig. 2 (although not necessarily drawn to scale). The horizontally aligned arrangement is shown in Fig. 2a. In this orientation, the clay sheets are parallel to the flat faces of the sample. Since thermal conductivity is measured across the thickness of the samples, the direction of heat flow is perpendicular to the planar clay layers, and thermal transport follows a complicated path through the thin struts connecting the layers and/or through the air pockets within the material. Fig. 2b illustrates a vertically aligned clay aerogel sample. Here, the clay sheets span the thickness of the sample, and in addition to transport across air pockets and/or interfaces, the heat can also flow uninterrupted along entire sheets within the aerogel. In both configurations, the spacing between clay sheets is around 20 microns and the thickness of the sheets is 0.1–1 microns. The struts are actually rarely observed under SEM since they are relatively infrequent, suggesting an even more open structure than depicted in Fig. 2. Lower magnification SEM images display no obvious struts over spans greater than 2 mm. For modeling purposes, the spacing between struts is assumed to be infinite.

In addition to varying the geometrical configuration, the effect of polymer inclusion within an aerogel structure with a vertical orientation (Fig. 2b) is also examined. The addition of 108,000 Da molecular weight poly(vinyl alcohol) (PVOH) is made to the water–clay mixture before freezing. In the dried sample, the polymer infiltrates and/or coats the clay in the aerogel framework. The presence of the polymer lends mechanical rigidity to the structure. The amount of polymer in the clay–polymer blend, and thus the resulting sample rigidity, can be controlled by changing the concentration of PVOH added to clay–water solution in processing. The increasing rigidity can be seen in the reduced tendency of the samples to break during handling. The rigidity also can be affected, to lesser degree, by varying the molecular weight of PVOH used.

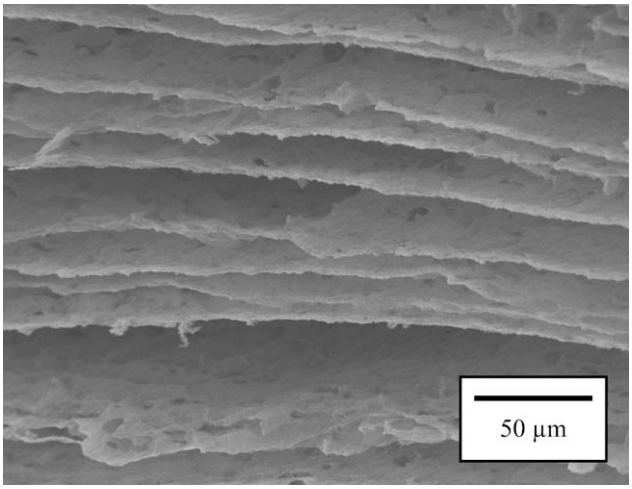

Fig. 1. Representative SEM image of clay aerogel structure.

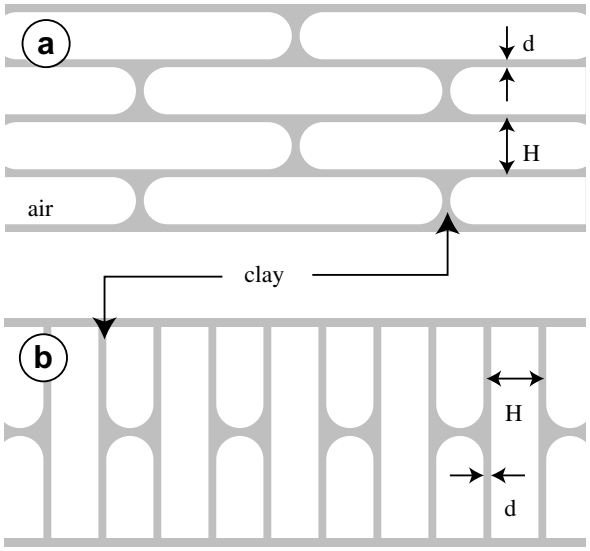

Fig. 2. Structure of the aerogel samples: (a) horizontally aligned, (b) vertically aligned.

Table 1
Water content on a mass basis, density, and internal dimensions (layer thickness, d, and interlayer spacing, H) of the clay aerogel samples

Configuration	Water content (%)	Density (kg/m^3)	d (μm)	H (μm)
Horizontal	7.7	~50	0.33	15
Vertical	6.5	35	0.3	20
Polymer (vert.)	3.7	68	0.9	20

Each of the three aerogel samples was characterized in terms of internal geometrical dimensions and water content. The internal geometry is determined using a combination of scanning-electron micrographs (Phillips XL-30 ESEM) and bulk sample density measurements. The bulk density is determined by weighing the samples and measuring their external dimensions with a micrometer. The water content in the samples is measured via thermogravimetric analysis (Mettler-Toledo TGA-SDTA851e). It is assumed that the internal pores of the clay aerogel are primarily open in character such that the majority of any residual water is expelled during thermogravimetric testing. Modeling the heat flow through these materials requires knowledge of the internal dimensions as well as the thermal conductivity of the clay. Clay thermal conductivity tends to increase with the amount of absorbed water in the clay [13] so a measurement of the water content is necessary to determine the conductivity of the clay forming the aerogel structure.

The results of the structural aerogel characterization are summarized in Table 1. The level of water absorption measured in each of the aerogel specimens is used to select a representative value for the thermal conductivity of the clay based on previous data collected by Penner et al. [13]. The clay thermal conductivity is a required input to the thermal model as discussed in more detail later. The decrease in water content from ~7% to ~3.7% with the addition of the polymer to the aerogel probably reflects the greater hydrophilicity of clay than polymer in this system.

The measured bulk density values are consistent with measurements of previous aerogel samples [12]. The increased density of the PVOH sample is the result of the increased layer thickness, d, with little change in the interlayer spacing, H. As seen in SEM images (not shown), the polymer blends with the clay forming an expanded structure that fills more of the interlayer void.

The distance between clay sheets is determined directly from SEM images of each of the samples. For all of the aerogel specimens, this spacing is around 20 μm. The thickness of the clay layers is found indirectly from the density measurements and the interlayer spacing assuming an idealized geometry as in Fig. 2 with the distance between struts tending to infinity. This calculation leads to a layer thickness of around 0.3 μm for the polymer-free samples. The incorporation of PVOH leads to a layer thickness approximately three times larger.

2.2. Thermal measurement

The thermal conductivity of the aerogel is measured with a conventional heat flow meter setup based on ASTM C 518 [14] as shown in Fig. 3. This method provides a simple means of determining the integrated effective thermal conductivity of a sample of realistic practical dimensions. It works well for relatively low (<0.1 W/mK) thermal conductivity materials. The aerogel sample ($7.6 \times 7.6 \times 0.6$ cm) is inserted between two plates of the same known material, in this case poly(vinyl chloride) (PVC). The sample is compressed slightly to minimize the effect of thermal contact resistance. The measurement system was calibrated using three low conductivity reference samples (cellulose, fiberglass, and semi-rigid PVC foam insulation) in place of the aerogel. These materials have thermal conductivities 1.3, 1.7, and 1.4 times larger than air, respectively. The calibration resulted in an effective conductivity for the PVC plates of 0.10 W/mK. Heat is sent through these three layers in a one-dimensional manner by utilizing high aspect ratio reference plates and samples (area to thickness is maintained at least ten to one) and evenly distributing the heat from the heater via a heater spreader. Further, the setup is thermally insulated around the sides of the stack and over the heater to encourage one-dimensional conduction through the stack. The temperature drop across each of the three sections is measured using four thermocouples, each located along the centerline of the stack. Note that grooves were formed in the PVC plates into which the thermocouples were placed to eliminate the gap that would have otherwise formed due to the presence of the thermocouple bead. For one-dimensional heat flow, the rate of heat transfer Q through each layer is given by Fourier's Law,

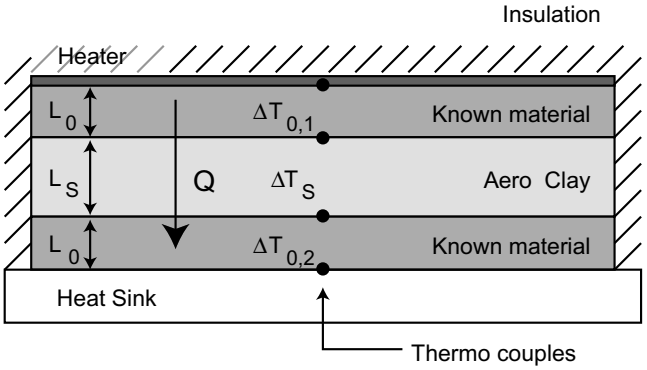

Fig. 3. Schematic of the heat flow meter setup for thermal conductivity measurement.

$$Q = kA\frac{\Delta T}{L}. \tag{1}$$

If conduction is truly one-dimensional (no heat is lost through the sides), the heat transfer rate is identical for all three layers and the temperature drop across both of the known plates would be the same since they have the same thickness, L_0. For the actual test device, the difference in these temperature drops ($\Delta T_{0,1}, \Delta T_{0,2}$) gives a measure of the accuracy of the one-dimensional heat flow approximation. In determining the thermal conductivity, the two temperature drops across the known pieces are averaged. This gives a good measure of the true heat flux through the aerogel sample; the actual rate of heat transfer through the sample will be between the values of the two reference materials.

The thermal conductivity of the sample k_s is measured relative to that of the known material, k_0, and is given as a combination of the thicknesses and temperature drops across the two different materials as

$$\frac{k_s}{k_0} = \frac{\Delta T_0}{\Delta T_s}\frac{L_s}{L_0}, \tag{2}$$

where ΔT_0 is the average of $\Delta T_{0,1}$ and $\Delta T_{0,2}$. Eq. (2) assumes that the heat flux is the same through the sample and reference material.

A constant heat flux is applied until the four temperatures reach steady-state values (about 12 h). After this time, the three temperature drops are measured over a period of at least an hour. The difference in the temperature drops between each of the known material sections was around 2% for the tests, ensuring that the conduction is sufficiently one-dimensional. All measurements were made at a mean sample temperature of approximately 30 °C.

2.3. Effective conductivity model

An analytical model was developed to provide insight into thermal transport in these unique materials and to enable prediction of

how various system characteristics might influence thermal transport. Dimensions of conventional aerogels are typically in the nanometer range, and therefore previous modeling attempts [15,16] have included non-continuum effects. Nonetheless for this modeling effort, the characteristic dimensions are at the microscale, and consequently thermal conductivities for the individual components of the aerogel (i.e. air and clay) are taken at their bulk values; a continuum model is capable of predicting the heat flow through the material.

To create the analytical model, a specific repeating geometric representation of the clay aerogel structure is considered as shown in Fig. 4. For horizontally aligned samples heat flow is from top to bottom in the sketch as shown by Q_H. From the perspective of the geometrical representation, heat effectively flows from left to right in consideration of the vertically aligned samples, denoted Q_V. Since the aerogel structure is periodic, it is sufficient to consider a single repeat cell when calculating the effective thermal conductivity. One such cell is highlighted in Fig. 4. This repeat cell is clearly non-symmetrical leading to different thermal conductivities in each of the two alignment directions.

The effective thermal conductivity of the aerogel sample is found by summing the thermal resistances in each dissimilar region of the cell. The heat fluxes for each unique heat transfer path are added assuming a single temperature difference ΔT across the cell thickness in a manner following Ref. 16. By Fourier's law, the effective thermal conductivity k_{eff} is given in terms of this total heat transfer rate Q_{tot} and the cell area perpendicular to heat flow A_{tot} and thickness L_{tot} as

$$k_{eff} = \frac{Q_{tot} L_{tot}}{A_{tot} \Delta T}. \tag{3}$$

In the horizontal configuration (vertical heat flow Q_H in Fig. 4), there are two unique heat paths: one that includes the struts connecting the clay sheets, one that does not. The sum of these two heat flows gives the total heat transfer rate Q_H for horizontally aligned samples

$$Q_H = 2Bd\frac{k_c k_a \Delta T}{(2d+H)k_a + Hk_c} + (W-d)B\frac{k_c k_a \Delta T}{2dk_a + 2Hk_c}, \tag{4}$$

where B is the depth of the sample (into the plane) and k_c and k_a are thermal conductivities of the clay and air, respectively. The first term in Eq. (4) corresponds to the heat flow that includes the struts. The second terms describes the heat flow through the clay sheets and air pockets away from the struts. The effective thermal conductivity for horizontally aligned samples, k_H, in terms of the air conductivity is then

$$\frac{k_H}{k_a} = \frac{H/d+1}{W/d+1}\left[\frac{4(k_c/k_a)}{(H/d+2)+(H/d)(k_c/k_a)} + (W/d-1)\frac{(k_c/k_a)}{(H/d)(k_c/k_a)+1}\right] \tag{5}$$

based on an area $A_{tot} = (W + d)B$ and a total thickness $L_{tot} = 2(H + d)$.

An identical procedure in the other direction leads to the effective conductivity for vertically aligned samples, k_V.

$$\frac{k_V}{k_a} = \frac{W/d+1}{H/d+1}\left[(k_c/k_a)\frac{1}{W/d+1} + (k_c/k_a)\frac{H/d}{(W/d)(k_c/k_a)+1}\right] \tag{6}$$

In the horizontal alignment, an additional term is added to account for radiation that contributes to the experimentally measured conductivities. Radiation is modeled using the diffusion method with a Rosseland mean absorption coefficient [17]. This method formulates the radiative heat flux vector as a temperature gradient multiplied by a radiative thermal conductivity, k_{rad}. For porous materials, the radiative conductivity is given by [18],

$$k_{rad} = \frac{16n^2\sigma T_{rad}^3}{3\rho_{eff}K/\rho_c} \tag{7}$$

where n is the refractive index, σ is the Stefan–Boltzmann constant, T_{rad} is the mean temperature in the aerogel, ρ_{eff} is the effective density of the clay aerogel, and K/ρ_c is the specific extinction coefficient of the clay. A representative value of 60 m^2/kg is taken for the specific extinction coefficient from those listed in Ref. [14]. A value of one is used for the refractive index. The effective density is measured directly and is related to the internal geometry (Fig. 4) as

$$\rho_{eff} = \frac{\rho_c d(W+d+H) + \rho_a HW}{(W+d)(H+d)}. \tag{8}$$

3. Results and discussion

Using the heat flow meter described above, the thermal conductivity of three different aerogel samples was measured. These measurements are shown in Fig. 5 as a function of clay layer spacing to the clay layer thickness ratio, H/d. The experimental results are plotted together with the corresponding curves from the effective conductivity model. The samples consisted of: one horizontally aligned, one vertically aligned, and one vertically aligned with

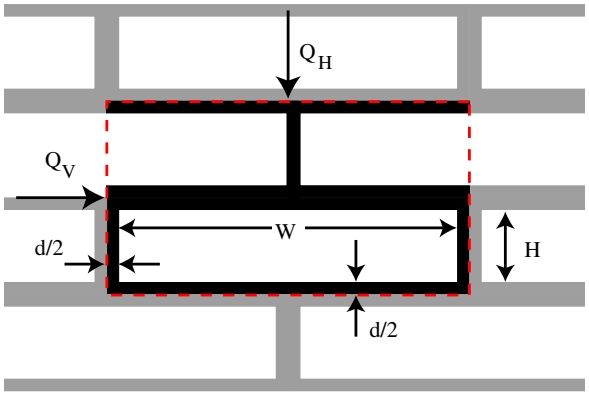

Fig. 4. Theoretical idealization of the aerogel structure.

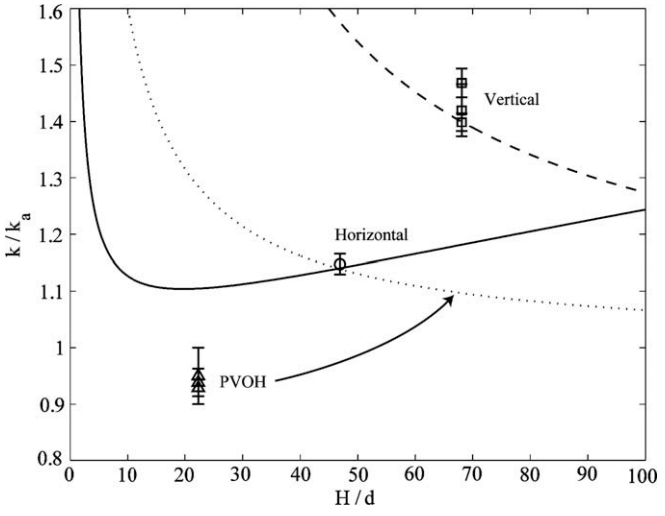

Fig. 5. Thermal conductivity of aerogel samples normalized by the conductivity of air as a function of the clay layer spacing to clay layer thickness ratio, H/d. Experimental results represented by the data points. Curves indicate the results from the effective conductivity theory for an infinite cell width, W. Sample configurations include horizontal (circle, solid line), vertical (square, dashed line), and vertical with PVOH added during aerogel processing (triangle, dotted).

PVOH added. Multiple data points correspond to repeated tests of the same sample. The error bars account for the experimental uncertainties in the sample thickness, the thermocouple readings, and the value of the thermal conductivity of the reference material.

For all of the samples, the measured thermal conductivity is much closer to that of air than clay or PVOH as a consequence of the high porosity in the clay aerogel materials. Bulk clay and PVOH would have magnitudes of 29 and 8, respectively, when normalized by the conductivity of air. The results are consistent with measurements of conventional aerogels in that that they approach the thermal properties of air. Conventional aerogel materials have conductivities close to air and in some cases below air if their internal dimensions are small enough to limit the mean free path of air [15].

As expected, the vertically aligned aerogel specimen has a higher thermal conductivity than the horizontally aligned sample. In the vertical configuration the sheets of the aerogel structure are aligned with the applied heat flux. These sheets provide a continuous, relatively high thermal conduction path for the heat to flow. The conduction along the sheets leads to a significant increase over conduction through the air pockets alone. In contrast, heat flows perpendicular to the planar structure of the aerogel for the horizontally aligned sample. Heat is forced to flow either through the low conductivity air pockets between the sheets or through the thin, sparse struts connecting the sheets. The effective conductivity model shows that heat flows preferentially through the air pockets even for modest, rather than infinite, strut separation. Despite the higher thermal conductivity in the struts, their narrow width and discontinuous nature lead to a thermal resistance that is larger than in the air pockets. In the model, this is evidenced by the fact that the effective conductivity in the horizontal configuration is unchanged by changes to the clay thermal conductivity value as large as 10%. Lacking a significant conduction path through the clay, the thermal conductivity in the horizontally aligned aerogel is dominated by the conductivity through the air. This leads to a lower measured conductivity relative to the vertically aligned specimen. The effective conductivity theory fits well with the results from both of the samples without PVOH.

The thermal conductivity in the aerogel sample with embedded PVOH is unexpectedly lower than both the vertically aligned and horizontally aligned specimens without polymer. The presence of the polymer was expected to increase rather than decrease the thermal conductivity by filling voids that would have otherwise have been filled by air. Effective density measurements (Table 1) support this picture as the layer thickness of the aerogel specimen increases with polymer addition without significant change to the interlayer spacing. Moreover, the thermal conductivity of PVOH is 0.2 W/mK, a value between that for clay and air. Assuming that the clay–polymer blend has an effective conductivity between that of clay and PVOH, the effective conductivity model would predict a decrease in thermal conductivity compared to the vertical sample without polymer for a fixed H/d ratio. Even if the layer thickness was unaffected by polymer addition, the decrease in the conductivity of the clay–polymer blend would not be enough to match the reduction seen in the experimental data. The dotted effective conductivity curve in Fig. 5 is plotted using the conductivity of PVOH as the value for the clay–polymer blend. This value represents the limiting case of blending, but still fails to capture the reduction observed in experiments. Thus, the combination of clay and PVOH that makes up the aerogel structure must be such that the conductivity becomes lower than either of the constituents. This would be the case if the hybrid structure is more porous than either the clay or polymer alone. Future effort will focus on how varying concentrations of PVOH affect the structure and conductivity of the clay–polymer blended structure.

4. Conclusions

The physical and thermal properties of surfactant-free, clay-based aerogels were determined. SEM images show that the structure of these clay aerogels consists of a series of parallel clay sheets interconnected by sparse struts. The thermal conductivity of the clay aerogel samples was measured for two distinct geometrical configurations and with and without added poly(vinyl alcohol) during processing. The polymer enhances the mechanical strength of the clay aerogel. It was found that rather than increasing the thermal conductivity, the polymer actually decreases conductivity. Changes with sample orientation are well predicted by an effective thermal conductivity, whereas the model fails to predict the conductivity drop in the polymer sample. The cause of this conductivity reduction may be related to a more complex interaction between the polymer and clay than assumed in the current effective conductivity model.

Acknowledgement

Financial support from Aeroclay Inc. is greatly acknowledged. AeroClay™ is a registered trademark of Aeroclay Inc. for clay-based aerogel and aerogel composite products

References

[1] S.S. Kistler, Coherent expanded aerogels, J. Phys. Chem. 36 (1932) 52–64.
[2] K.I. Jensen, J.M. Schultz, F.H. Kristiansen, Development of windows based on highly insulating aerogel glazings, J. Non-Cryst. Solids 350 (2004) 351–357.
[3] M. Reim, W. Korner, J. Manara, S. Korder, M. Arduini-Schuster, H.-P. Ebert, J. Fricke, Silica aerogel granulate material for thermal insulation and daylighting, Sol. Energy 79 (2005) 131–139.
[4] J.E. Fesmire, Aerogel insulation systems for space launch applications, Cryogenics 46 (2006) 111–117.
[5] S.M. Jones, Aerogel: space exploration applications, J. Sol-Gel Sci. Technol. 40 (2006) 351–357.
[6] R.C. Mackenzie, Clay–water relationships, Nature 171 (1953) 681–683.
[7] F. Call, Preparation of dry clay-gels by freeze-drying, Nature 172 (1953) 126.
[8] H. van Olphen, Polyelectrolyte reinforced aerogels of clays-application as chromatographic adsorbents, Clay Miner. 15 (1967) 423–435.
[9] K. Norrish, J.A. Rausell-Colom, Effect of freezing on the swelling of clay minerals, Clay Miner. Bull. 5 (1962) 9–16.
[10] H. Nakazawa, H. Yamada, T. Fujita, Y. Ito, Texture control of clay-aerogel through the crystallization process of ice, Clay Sci. 6 (1987) 269–276.
[11] L.S. Somlai, S.A. Bandi, D.A. Schiraldi, L.J. Mathias, Facile processing of clays into organically-modifed aerogels, AIChE J. 52 (2006) 1162–1168.
[12] S. Bandi, M. Bell, D.A. Schiraldi, Temperature-responsive clay aerogel–polymer composites, Macromolecules 38 (2004) 6001–6003.
[13] E. Pennner, G.H. Johnston, L.E. Goodrich, Thermal conductivity laboratory studies of some Mackenzie highway soils, Can. Geotech. J. 12 (1975) 271–288.
[14] ASTM C 518-04, Standard test method for steady-state thermal transmission properties by means of the heat flow meter apparatus, ASTM International.
[15] L.W. Hrubesh, R.W. Pekala, Thermal properties of organic and inorganic aerogels, J. Mater. Res. 9 (1994) 731–738.
[16] S.Q. Zeng, A. Hunt, R. Greif, Geometric structure and thermal conductivity of porous medium silica aerogel, J. Heat Transfer 117 (1995) 1055–1058.
[17] R. Siegel, J.R. Howell, Thermal Radiation Heat Transfer, Hemisphere Publishing Corporation, Washington, 1981.
[18] R. Caps, J. Fricke, Aerogels. In: J. Fricke (Ed.), Proceedings of the First International Symposium, Springer-Verlag, New York, 1986.